PNAS RESEARCH ARTICLE | ENVIRONMENTAL SCIENCES
BIOPHYSICS AND COMPUTATIONAL BIOLOGY

A global estimate of multiecosystem photosynthesis losses under microplastic pollution

Ruijie Zhu[a], Zhaoying Zhang[b,c,d], Naichi Zhang[e,f], Huan Zhong[a,1], Fanqi Zhou[a], Xiao Zhang[a], Cun Liu[e], Yingnan Huang[e], Yuan Yuan[e,f], Yujun Wang[e], Chengjun Li[g], Huahong Shi[h], Matthias C. Rillig[i,j], Fei Dang[e,1], Hongqiang Ren[a], Yongguang Zhang[b,c,d], and Baoshan Xing[k]

Affiliations are included on p. 8.

Edited by Lewis H. Ziska, Columbia University, New York, NY; received November 17, 2024; accepted February 9, 2025 by Editorial Board Member Alan Hastings

Understanding how ecosystems respond to ubiquitous microplastic (MP) pollution is crucial for ensuring global food security. Here, we conduct a multiecosystem meta-analysis of 3,286 data points and reveal that MP exposure leads to a global reduction in photosynthesis of 7.05 to 12.12% in terrestrial plants, marine algae, and freshwater algae. These reductions align with those estimated by a constructed machine learning model using current MP pollution levels, showing that MP exposure reduces the chlorophyll content of photoautotrophs by 10.96 to 12.84%. Model estimates based on the identified MP-photosynthesis nexus indicate annual global losses of 4.11 to 13.52% (109.73 to 360.87 MT·y^{-1}) for main crops and 0.31 to 7.24% (147.52 to 3415.11 MT C·y^{-1}) for global aquatic net primary productivity induced by MPs. Under scenarios of efficient plastic mitigation, e.g., a ~13% global reduction in environmental MP levels, the MP-induced photosynthesis losses are estimated to decrease by ~30%, avoiding a global loss of 22.15 to 115.73 MT·y^{-1} in main crop production and 0.32 to 7.39 MT·y^{-1} in seafood production. These findings underscore the urgency of integrating plastic mitigation into global hunger and sustainability initiatives.

microplastic (MP) | meta-analysis | machine learning | photosynthesis reduction | global food safety

Humanity has been striving to increase primary productivity and thus food production to feed an ever-growing population. To achieve this, global initiatives are underway to expand arable land (1) and to enhance primary productivity (2). These ongoing efforts are now being jeopardized by plastic pollution (3) owing to its ubiquity and negative impact on food security, as recognized by the Food and Agriculture Organization (FAO) (4). Particularly, microplastics (MPs, less than 5 mm in size) have recently been suspected to take a toll on photosynthesis and, consequently, to primary productivity (5–8). Such a hidden nexus between MPs and photosynthesis, while far from clear, poses a potential threat to global efforts to achieve the United Nation's (UN's) Sustainable Development Goals (SDGs) 2, 3, 12, and 14, which aim to eradicate hunger, protect health, ensure sustainable consumption and production, and conserve marine resources for sustainable development.

Currently, there is a lack of consensus on the MP-photosynthesis nexus at the ecosystem or multiecosystem level, hampered by fragmented and sometimes contradictory results of individual studies. For instance, polystyrene MPs have been observed to exert negative effects on plant photosynthesis (9), while instances of minimal or even positive effects on plant photosynthesis have also been documented (10, 11). The responses of photosynthesis to MPs are further complicated by ecosystem complexity, exemplified by the diversity of environments they inhabit, and the wide range of photoautotrophs affected (e.g., plants and algae), together with the considerable heterogeneity of MPs themselves (12, 13). These complex factors make it difficult to extrapolate the results of individual studies on specific environmental conditions and photoautotrophic species to the ecosystem level (12). Therefore, a major challenge is to integrate quantitative and categorical data from these empirical studies in such a way that reliable predictions of the MP-photosynthesis nexus can be made at the ecosystem or multiecosystem level. Tackling these challenges would allow the estimate of regional and global food production under scenarios of MP pollution or mitigation, empowering decision-makers with information on the benefits of curbing plastic pollution. The information is important and timely for the ongoing negotiations on a plastics treaty at the UN and the forthcoming development of action plans and targets under the treaty.

Here, we aim to quantify the extent to which MPs affect photoautotrophic photosynthesis and subsequent primary productivity in terrestrial, marine, and freshwater ecosystems. We have used two independent approaches to capture ecosystem complexity, improve reliability, and pursue scientific rigor (14, 15). First, we utilize meta-analysis to integrate effect sizes

Significance

Our study presents a global assessment of microplastic pollution's impact on food security. By analyzing a comprehensive dataset of 3,286 records, we quantify the reduction in photosynthesis caused by microplastics across various ecosystems. This reduction is estimated to cause an annual loss of 109.73 to 360.87 million metric tons (MT) for crop production and 1.05 to 24.33 MT for seafood production. By reducing current environmental microplastic levels by 13%, these losses could be mitigated by 14.26 to 46.91 MT in crops and 0.14 to 3.16 MT in seafood. These findings underscore the urgency for effective plastic mitigation strategies and provide insights for international researchers and policymakers to safeguard global food supplies in the face of the growing plastic crisis.

The authors declare no competing interest.

This article is a PNAS Direct Submission. L.H.Z. is a guest editor invited by the Editorial Board.

[1]To whom correspondence may be addressed. Email: zhonghuan@nju.edu.cn or fdang@issas.ac.cn.

This article contains supporting information online at https://www.pnas.org/lookup/suppl/doi:10.1073/pnas.2423957122/-/DCSupplemental.

Published March 10, 2025.

derived from a database with a total of 3,286 observations compiled from 157 studies (*Materials and Methods* and *SI Appendix*, Fig. S1). This approach, based on the comprehensive up-to-date dataset, quantifies the overall effect of MPs on photosynthesis across empirical individual studies under diverse environmental conditions, but has the limitation of capturing the impacts of current MP pollution. To address that, we also establish MP-photosynthesis nexus using a machine learning (ML) modeling approach (16). By integrating current MP levels in the environment with the established MP-photosynthesis nexus, we estimate the impact of MPs on photosynthesis at the ecosystem level. Based on the quantified impacts, we then evaluate the cascading consequences on main crop production in terrestrial ecosystems and net primary productivity (NPP) in marine and freshwater ecosystems. Our results indicate a consistent negative impact of MPs on photoautotrophic photosynthesis in terrestrial, marine, and freshwater ecosystems, leading to significant reductions in global crop and seafood production. These previously unaccounted losses due to ongoing MP pollution pose a hidden yet persistent threat to global food security, highlighting the urgency of integrating plastic mitigation into global efforts to ensure a sustainable food supply.

Results and Discussion

MP-Induced Photosynthesis Reduction in Terrestrial, Marine, and Freshwater Ecosystems. The photosynthesis of terrestrial plants, marine algae, and freshwater algae exhibits an overall significant and negative response to the exposure of MPs, with effect sizes of photosynthesis ranging from −17.99 to −6.25% (mean: −12.12%), −12.34 to −1.75% (mean: −7.05%), and −14.32 to −4.16% (mean: −9.24%), respectively (Fig. 1). The responses do not vary significantly over different ecosystem types. The results are robust, with negligible publication bias of the analyzed dataset (*Materials and Methods* and *SI Appendix*, Text S1). Specifically, the total chlorophyll content and chlorophyll *a* content show strong and consistent declines (Fig. 1). These two parameters are key to photosynthesis (17, 18) and their contents are critical for predicting primary productivity of terrestrial and aquatic ecosystems, respectively (*Materials and Methods*). In contrast, the chlorophyll *b*, carotenoid, Fv/Fm ratio, and Y II reveal no consistent directional shift (*SI Appendix*, Fig. S2). In terrestrial ecosystems, total chlorophyll content decreases by 5.63 to 17.42% in plants (Fig. 1*A*). In aquatic ecosystems, the chlorophyll *a* content, which accounts for approximately three-quarters of the total chlorophyll content (19), decreases by 0.46 to 11.01% in marine algae and 7.80 to 18.25% in freshwater algae following MP exposure (Fig. 1 *B* and *C*).

Although the meta-analysis assesses the magnitude of the overall effect on photosynthesis across original individual studies, the results remain to be validated. To provide multiple lines of evidence, a ML approach is implemented. Among the five ML models constructed using the dataset collated from the meta-analysis (*SI Appendix*, Fig. S3), the Random Forest (RF) model is a robust and reliable tool that enables the prediction of photosynthesis inhibition, with the best prediction performance (R^2 = ~0.61, Fig. 2*A*). A dataset of current MP levels in terrestrial, marine, and freshwater ecosystems (Dataset S1) is then incorporated into the constructed RF model to obtain the predicted effect sizes. It is estimated that the current MP pollution would result in a reduction of 12.84% in total chlorophyll content for terrestrial plants, and a reduction of 10.96 and 12.57% in chlorophyll *a* content for marine algae and freshwater algae, respectively (Fig. 2*B*). Importantly, the magnitudes of photosynthesis inhibition responses predicted by the RF model align with those obtained from the meta-analysis, confirming the external validity of the meta-analysis results. The effect sizes for terrestrial plants and aquatic algae from the meta-analysis are thus utilized to estimate the global loss of primary productivity in terrestrial and global aquatic ecosystems (GAEs) (see next section).

To gain an insight into the inhibitory mechanisms of MPs on photosynthesis, we further investigate the drivers of reductions in photosynthesis using subgroup analysis in meta-analysis and the SHapley Additive exPlanations (SHAP) values in the RF model. Meta-analysis indicates that the significant drivers over different ecosystems are exposure concentration, MP size, exposure duration, MP type, and MP weathering ($P < 0.05$, *SI Appendix*, Figs. S4 and S5 and Table S1). The RF model reveals that photoautotrophic species, exposure concentration, MP size, and exposure duration are the most significant top feature variables based on the algorithms (Fig. 2 *C* and *D*). Importantly, the meta-analysis and the RF model approaches are consistent in identifying the key drivers of MP-induced photosynthesis reduction, including the size, exposure duration, and concentration of MPs, suggesting their vital role in mediating the MP-photosynthesis nexus (see further discussions in *SI Appendix*, Fig. S6 and Text S2). Interestingly, study site does not exert a considerable influence on photosynthesis responses, as confirmed by the results of both meta-analysis and ML approaches (Fig. 2 *C* and *D* and *SI Appendix*, Table S1). This generality of responses across sites suggests that the responses obtained can be

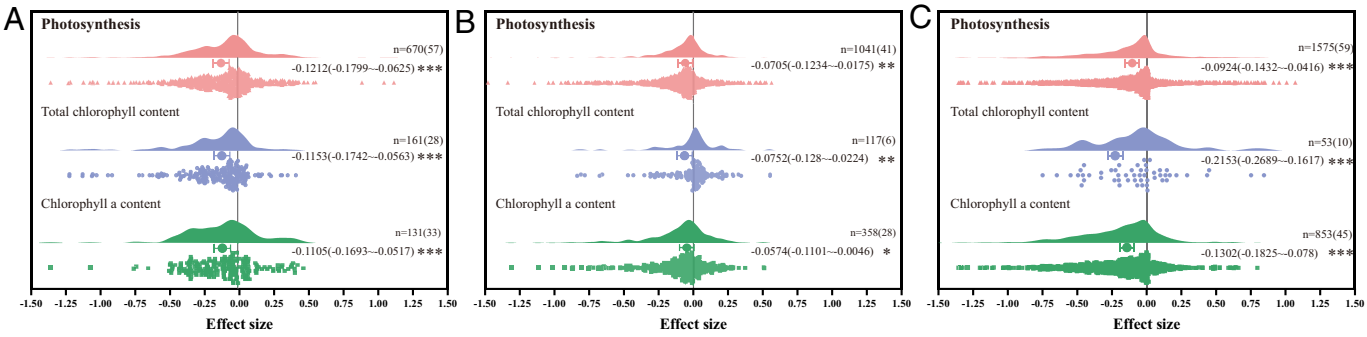

Fig. 1. Forest and raincloud plots of effect sizes on photosynthesis following MP exposure for terrestrial plants, marine algae, and freshwater algae. (*A*) terrestrial plants; (*B*) marine algae; (*C*) freshwater algae. The kernel density and jitter scatterplots show the distribution of observed effect sizes within the meta-database. Means (dots), 95% CI (CI, error bars), and n values (number of observations sourced from the number of studies in parentheses) are presented for the overall meta-analytic results (first row, Photosynthesis) and for other variables (total chlorophyll content and chlorophyll *a* content). Only total chlorophyll content and chlorophyll *a* content are presented because of their importance in photosynthesis and their use in the Soil Canopy Observation, Photochemistry, and Energy fluxes (SCOPE) model and the Vertically Generalized Production Model (VGPM). Other photosynthesis variables are shown in *SI Appendix*, Fig. S2. The value of the effect size is significant if the 95% CI does not overlap zero. Significance codes: ***$P < 0.001$, **$P < 0.01$, *$P < 0.05$.

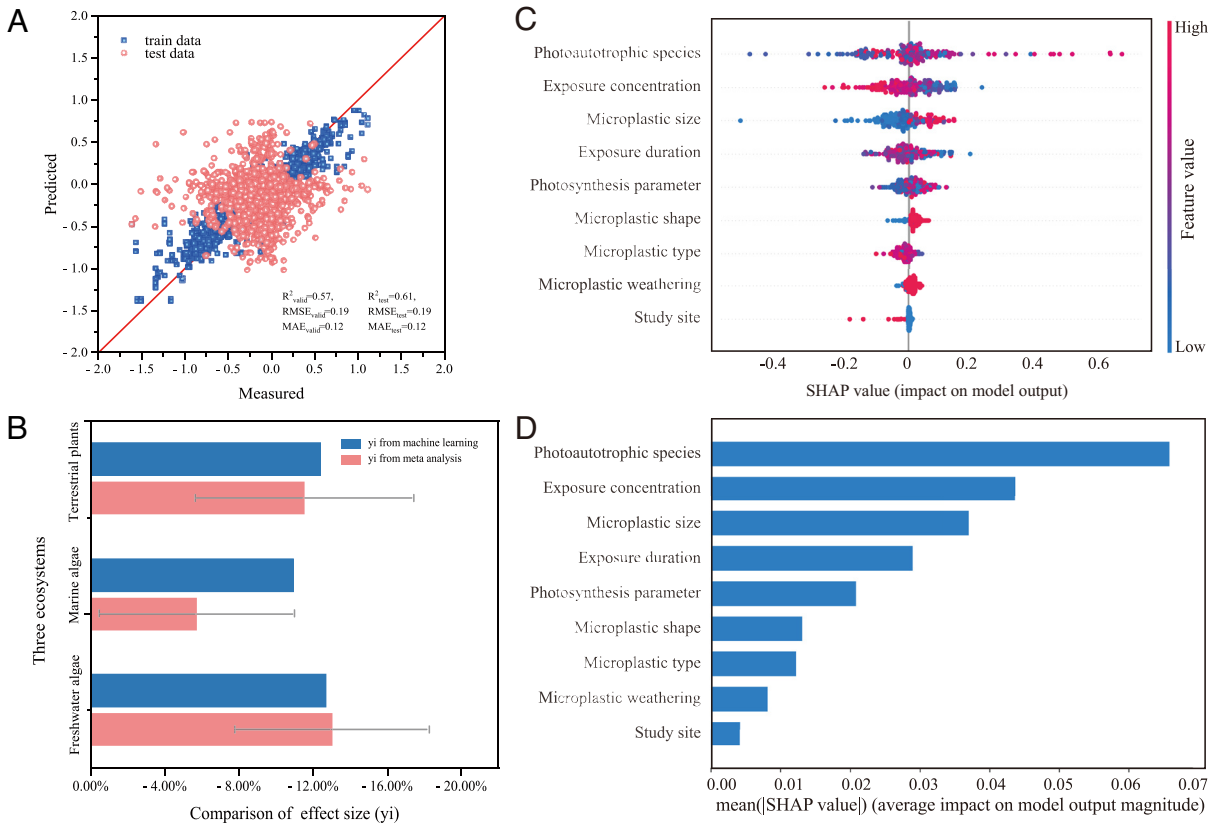

Fig. 2. Performance and predicted effect size (yi) of the RF model. (*A*) measured versus predicted effect size using the RF model, with blue square markers as the training set and red dot markers as the test set. The 1:1 predicted-to-observed relationship is represented by the solid red line. The mean R^2, RMSE, and mean absolute error (MAE) of the training and test data are also shown. (*B*) comparisons of effect sizes obtained from the RF model and the meta-analysis for terrestrial, marine, and freshwater ecosystems. The effect sizes from the RF model (blue) were projected based on the environmental dataset of field MP pollution from three ecosystems in Europe and North America. The estimated effect sizes from the meta-analysis are shown with mean values (red bars) with their 95% CI (gray error bars). The effect sizes of total chlorophyll content in terrestrial plants, and of chlorophyll *a* content in aquatic algae were predicted, because they are input parameters of the SCOPE model and VGPM. (*C*) the importance of parameters affecting the RF model output using SHAP. The top nine influential features are sorted based on the maximum absolute value of the SHAP values. The SHAP values on the *x*-axis indicate the feature values and their impact, either positive or negative, on the prediction of the effect size. (*D*) average impact (mean |SHAP| value) and importance ranking of different input parameters on model output magnitude in the RF model.

extrapolated to any described (or undescribed) area to estimate primary productivity losses following MP exposure.

MP-Induced Photosynthesis Reduces Global Crop and Seafood Production. We then estimate the cascading effects of MPs on food production losses, based on the quantified MP-photosynthesis nexus and existing models that bridge photosynthesis and primary productivity. Specifically, SCOPE model, a global simulation model based on total chlorophyll content on a pixel basis (0.083° × 0.083°), has been extensively employed in simulating gross primary productivity (GPP) in the terrestrial biosphere (20) and is used here to translate reduced photosynthesis into decreased primary productivity (details in *Materials and Methods*). MP exposure reduces the total chlorophyll content by 5.63 to 17.42% (Figs. 1 *A* and 2 *B*), resulting in a loss of approximately 109.73 to 360.87 MT·y^{-1} in the global production of rice, wheat, and maize (Fig. 3), without considering the potential effects of MP on other parameters in the SCOPE model. Such a loss represents 4.11 to 13.52% (median: 9.56%) of the total annual global production of these crops, with significant implications for food security.

Among the three main crops, maize is subject to substantial worldwide losses, with estimated loss ranging from 48.92 to 161.58 MT·y^{-1} (*SI Appendix*, Table S2). The decline in maize production following MP exposure may be attributed to the formation of flavonoids, which scavenge MP-induced reactive oxygen species. This unbalances the trade-off between growth- and defense-related metabolism, resulting in a reduction in maize growth (21, 22). As for rice and wheat, the estimated total global losses are 26.71 to 87.97 MT·y^{-1} and 34.10 to 111.32 MT·y^{-1}, respectively.

Regionally, we find that MP-induced losses are considerably higher in Asia, North America, and Europe (Fig. 3). In Asia, a total of 53.82 to 177.14 MT·y^{-1} of main crops, including 23.87 to 78.66 MT·y^{-1} of rice, are projected to be lost due to MP pollution. These losses represent 49 and 89% of global crop and rice losses, respectively (Fig. 3*A* and *SI Appendix*, Table S2). In North America, the projected losses of 20.42 to 67.79 MT·y^{-1} of main crops, of which maize accounts for 15.69 to 52.26 MT·y^{-1}, represent 19 and 32% of the global main crop and maize losses, respectively (Fig. 3*C* and *SI Appendix*, Table S2). In Europe, the estimated losses of main crops are 17.32 to 56.82 MT·y^{-1}, with 11.23 to 36.79 MT·y^{-1} of wheat to be lost. Those losses represent 16 and 33% of global losses of main crops and wheat, respectively (Fig. 3*B* and *SI Appendix*, Table S2). Conversely, South America, Africa, and Oceania have markedly lower losses than Asia, North America, or Europe (*SI Appendix*, Table S2 and S3). This may be attributed to the relatively low level of crop production in these regions and/or the paucity of data in MP contamination (23–25).

Importantly, our results suggest that MP-induced crop losses are exacerbating global food insecurity. Utilizing the data of global food supply and population growth rates (details in *Materials and Methods*), it is estimated that under the business-as-usual scenario, future production levels of main crops will meet the global demand

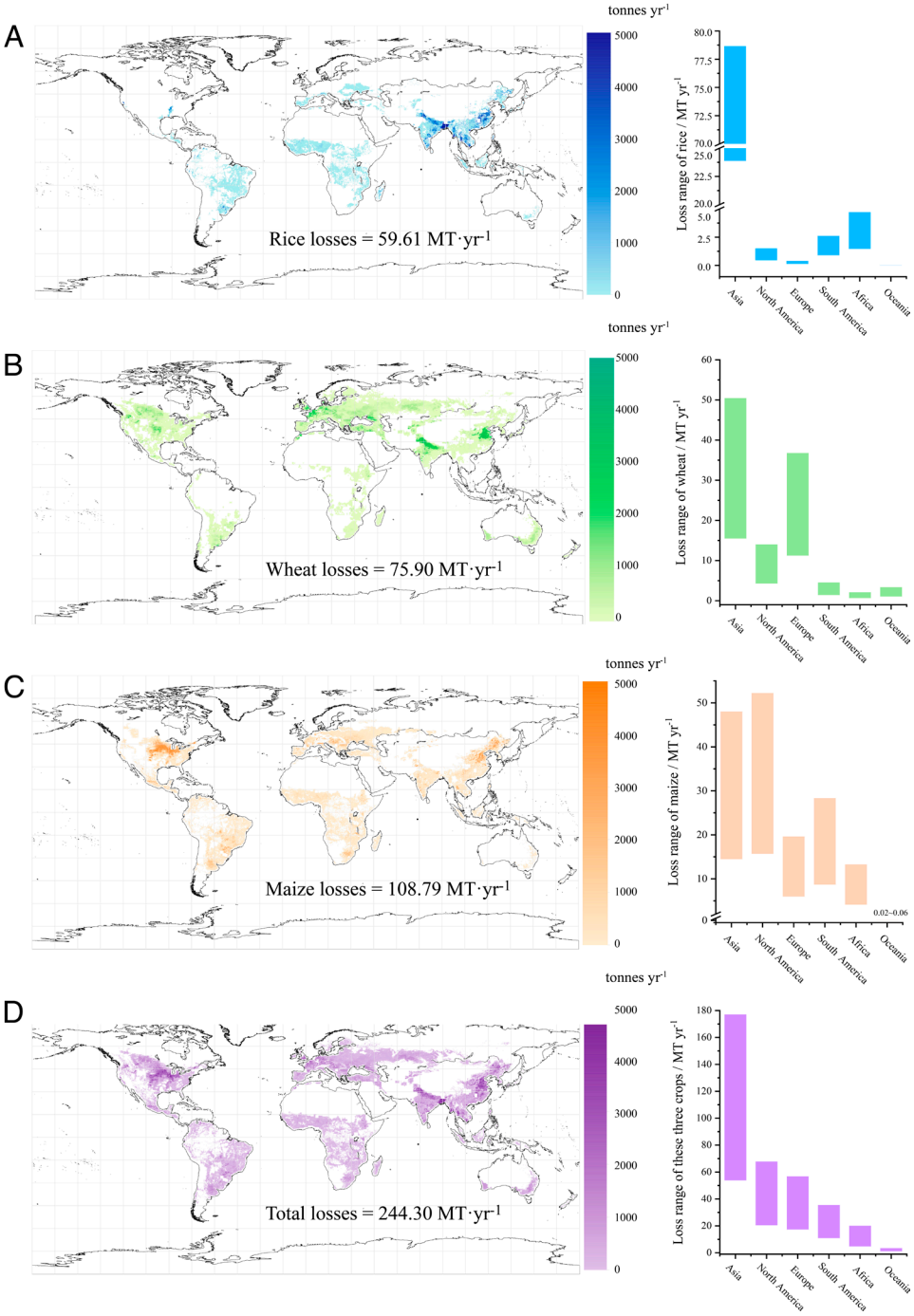

Fig. 3. Global maps of annual production losses for three main food crops. (*A*) rice; (*B*) wheat; (*C*) maize; (*D*) three crops combined. The maps on the left display the median value of the predicted annual production losses, while the floating bar charts on the right illustrate the range of annual losses for the corresponding crop. Crop production data for the 2020 version were obtained from the Spatial Production Allocation Model (SPAM) database. Crop production losses were obtained using the SCOPE model, which was used to simulate the GPP without (GPP_{ref}) and with (GPP_{exp}) MP exposure. The reduction in crop production was estimated based on the fact that the loss percentage of crop production is equal to that of GPP, described as ($GPP_{ref} - GPP_{exp}$) /GPP_{ref}. Please refer to Eq. **5** in Materials and Methods for more details. The spatial resolution of the calculations is 0.083° × 0.083°. MT, million tonnes.

projections (*SI Appendix*, Fig. S7A). However, MP exposure reduces photosynthesis and thus crop production, thereby undermining global food supply (*SI Appendix*, Fig. S7*A*). Indeed, the magnitude of annual crop losses caused by MPs (9.56%) is comparable to the losses (~10%) caused by climate change in 1964–2008 (26–28), extreme precipitation in 1999–2012 (29), or drought under Representative Concentration Pathway 2.6 (*SI Appendix*, Table S4) (30). In 2022, between 691 and 783 million individuals were affected by hunger as a consequence of conflicts, climate extremes, economic shocks, and growing inequality (31). MP exposure is expected to exacerbate this crisis, with a net increase of hundreds of millions of people estimated to be at risk of starvation worldwide (*SI Appendix*, Fig. S8). The threat posed by MPs to food security is further compounded by the accumulation of MPs in foods such as crops and vegetables (32), resulting in dietary exposure and health risks (33). A more alarming scenario is that such adverse effects on global food security may increase over time as MPs accumulate in soils, given the key role of MP concentrations in inhibiting photosynthesis (Fig. 2*D* and *SI Appendix*, Fig. S5), thereby amplifying the threat to sustainable

crop supply and human health. Consequently, MP-induced photosynthesis losses have been and will continue to be a direct challenge to achieving SDG goals 2, 3, and 12.

In GAEs, including marine and freshwater ecosystems, MP exposure results in a loss of 147.52 to 3415.11 MT C·y^{-1}, equivalent to 0.31 to 7.24% of the total NPP in these ecosystems (Fig. 4 and *SI Appendix*, Fig. S10). This loss is estimated using a VGPM in combination with data collected by the MODIS sensor (details in *Materials and Methods*), based on a 0.46 to 11.01% reduction in chlorophyll *a* content in marine algae (Figs. 1 *B* and 2 *B*), which account for over 99.5% of global algal production (34). The reduction in NPP could result in a decrease in fish and seafood production at the higher trophic levels by approximately 1.05 to 24.33 MT·y^{-1} (*SI Appendix*, Fig. S9*A* and Table S5). Such loss of fish and other seafood products incurs a protein loss of 0.59 to 2.70 MT·y^{-1} (*SI Appendix*, Fig. S9*B* and Table S5), which is adequate to feed 26.85 to 123.10 million adults (with a body weight of 75 kg) based on the recommended daily protein intake of 0.8 g kg^{-1} by the United States Department of Agriculture and the World Health Organization (35, 36). Collectively, our results highlight the previously unrecognized role of MPs in threatening seafood security and contributing to hidden hunger particularly in coastal communities that rely heavily on seafood (34, 37), thereby jeopardizing SDG goals 2 and 14, i.e., zero hunger and the sustainable use of marine resources.

Importantly, these adverse effects are highly likely to extend from food security to planetary health, as photosynthesis and, consequently, primary productivity serve as the foundation for not only food supply for humans but also key ecological functions. These include nutrient cycling and ecosystem biomass allocation (38), soil carbon storage and turnover (38, 39), and the potential for ocean carbon sequestration (40), given that phytoplankton photosynthesis contributes to nearly half of the global annual carbon dioxide fixation (41, 42). Moreover, the reduction in primary productivity leads to an imbalance in predator–prey relationships and overall ecosystem instability (43). The cumulative effects of reduced primary productivity and trophic cascades have implications for ecological functions, carbon cycling, and the provision of ecosystem services.

By integrating meta-analysis and ML approaches, we demonstrate the photosynthesis responses of terrestrial plants, and marine and freshwater algae to MPs, as well as the downstream consequences on global loss of crop production, aquatic NPP, and seafood production. We have screened, compiled, and analyzed all available dataset, incorporating uncertainties into our assessment processes using probabilistic approaches. We have utilized two independent approaches (meta-analysis and ML models) to ensure consistency and scientific rigor. We acknowledge that our estimation of the quantitative responses of photosynthesis, and hence NPP, to MP exposure has potential limitations, e.g., uncertainties in evaluating ecosystem photosynthesis losses using the currently insufficient dataset, lack of continually updated data for estimating primary productivity losses, and gaps in our knowledge of the MP-photosynthesis nexus (see further discussions in *SI Appendix*, Text S3). A conceptual framework has been designed to facilitate the continual updating of data input to the analysis process (*SI Appendix*, Fig. S11). As more raw data on the MP-photosynthesis nexus become available from field studies and a continuous process of updating and optimizing the temporal scope of remote sensing data is implemented, our model's precision and accuracy can be ameliorated through training and calibration (*SI Appendix*, Fig. S11). Nevertheless, the estimated impacts at the ecosystem or planetary level highlight the urgency of considering MP pollution in the context of global food security, which is already under pressure from climate change and biodiversity loss (44, 45). The generality of MP-induced photosynthesis inhibition across multiecosystems provides a foundation for developing a predictive understanding of the loss of primary productivity, which is concerning for environmental and human health. Meanwhile, these results suggest promising scenarios where ongoing and forthcoming efforts to mitigate plastic pollution would alleviate the global loss of crop and seafood production, as discussed below.

Mitigation of MP Pollution Alleviates Global Losses of Crop and Seafood Production. Here, on a planetary scale, we predict the overall photosynthesis responses of terrestrial, marine, and freshwater ecosystems to projected MP mitigation, as indicated by the decreases

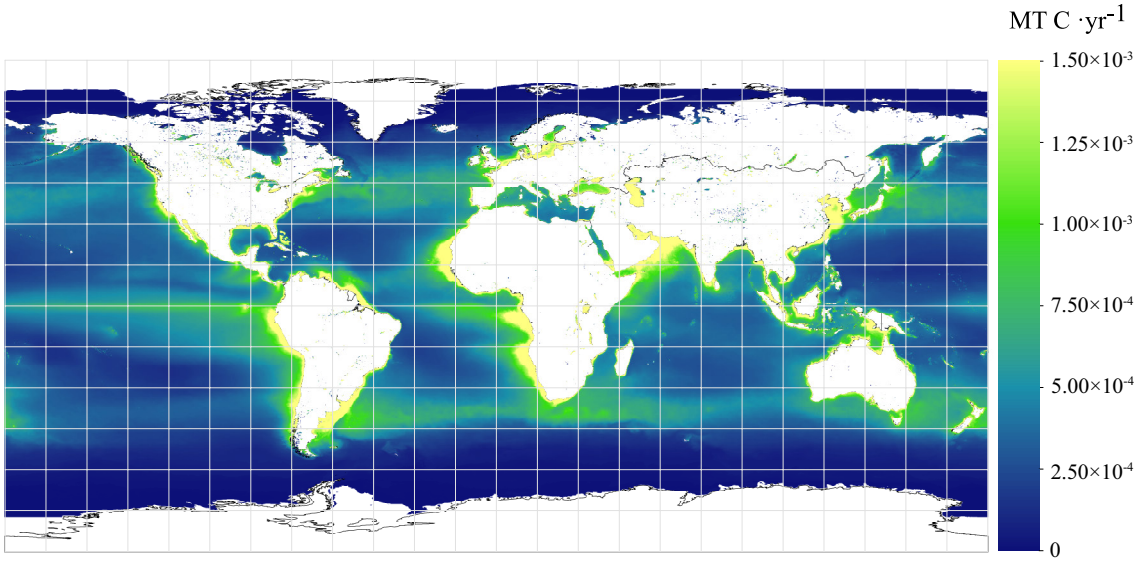

Fig. 4. Projected annual NPP losses of GAEs. The VGPM was used to simulate the average NPP loss from 2017 to 2022 following MP exposure. The spatial resolution of the calculations is 0.083° × 0.083°. Input data for satellite ocean color remote sensing were sourced from the MODIS sensor. The annual loss of NPP was estimated to be between 147.52 and 3415.11 MT C·y^{-1}, representing 0.31 to 7.24% of the global annual total NPP (*SI Appendix*, Fig. S10). The figure presents the median value of NPP losses. MT C, million tonnes of carbon.

in environmental MP concentration. The prediction is centered on the fact that the MP concentration is a key driver of photosynthesis inhibition (Fig. 2*D*) and is expected to decrease under global plastic mitigation efforts. These efforts include but are not limited to i) reducing the use of plastics and their discharge into the environment, with reported reductions of up to 50% (46), and ii) developing and deploying novel technologies to reduce the concentration of plastic debris in the environment, with efficiencies of up to 15% for conventional plastics and 65% for bioplastics (see further information and discussions in *SI Appendix*, Text S4 and Table S6).

Based on these documented reductions in plastic use and discharge, and degradation efficiencies, we set up four distinct projections of reductions in environmental MP concentrations: business-as-usual, lower range of projections (1 to 20%) (46), intermediate projections (21 to 40%) (47), and higher projections (41 to 50%) (3), though potential uncertainties remain in estimating mitigation scenarios (see further discussions in *SI Appendix*, Text S5). Our analysis suggests that, on a global scale, photosynthesis responds nonlinearly to the reductions in environmental MP concentration (*SI Appendix*, Fig. S12). Under scenarios where reductions in environmental MP concentration fall within the lower range of projections (1 to 20%), global photosynthesis losses are expected to be reduced by 1.3 to 38.1%, as compared to the business-as-usual scenario. For example, a 12.6% reduction in MP concentration could reduce global photosynthesis losses by 30% (*SI Appendix*, Fig. S12). This in turn would reduce the losses by 22.15 to 115.73 $MT{\cdot}y^{-1}$ for main crops such as rice, wheat, and maize, corresponding to USD 6,477 to 33,870 million in agricultural production value. Similarly, a 12.6% decrease in MP concentrations within aquatic environments could mitigate losses in seafood production by 0.32 to 7.39 $MT{\cdot}y^{-1}$, corresponding to a reduction in protein loss of 0.04 to 0.68 $MT{\cdot}y^{-1}$. Further declines in environmental MP levels to intermediate projections (21 to 40%) and higher projections (41 to 50%) would result in reductions in global photosynthesis losses of 39.1 to 54.2% and 54.9 to 60.6%, respectively, in comparison to the business-as-usual scenario. These preliminary estimates highlight the potential for securing the global food supply by reducing MP levels in the environment and emphasize the importance of aligning ongoing efforts to mitigate plastic pollution with strengthening food safety systems.

Overall, our results demonstrate the ecosystem- and planet-level impact of MP pollution on photosynthesis, highlighting a major threat from MPs to global primary productivity. The cascading consequences of the pervasive MP-induced inhibition of photosynthesis for species at higher trophic levels, including humans, include not only increased food insecurity, but also imbalances in predator–prey relationships and overall ecosystem instability. These could threaten global food security and the health of ecosystems already under immense pressure from global change and intensifying human activities. Integrating our findings into broader sustainable development frameworks can inform treaty negotiations and contribute to achieving the UN SDGs and addressing the pressing challenge of feeding a growing global population in a world increasingly impacted by the triple planetary crisis of environmental pollution, climate change, and biodiversity loss (48). Importantly, the estimated benefits of plastic mitigation in alleviating the global loss of food production pave a pathway of aligning the forthcoming plastic treaty with global initiatives to achieve the SDGs, particularly those concerning food, health, and sustainable development (49).

Materials and Methods

Meta-Analysis.

Literature search. Relevant literature was identified using keyword searches in ISI Web of Science Core Collection database until 6th June, 2024, focusing on the impacts of MPs on the photosynthesis of plants and algae (the search terms listed in *SI Appendix*, Text S6). To be included in the meta-analysis, predefined criteria for studies were established to ensure quality control: i) at least one of the photosynthesis-related parameters (*effect size calculation*) was reported; ii) a control group not exposed to MPs and treatment groups with MP exposure were included; iii) each photosynthesis-related parameter was documented in three or more publications; iv) data on means, estimation of variation, and sample sizes ($n \geq 3$) were reported; and v) details on the type, size, exposure duration, and exposure concentration of MPs were provided. The initial search yielded 6,808 studies, with 157 studies meeting all aforementioned criteria. Further details are provided in *SI Appendix*, Text S6 and in the PRISMA flowchart (*SI Appendix*, Fig. S1). The Get-data Graph Digitizer 2.26 software was used for extracting data from figures. If only box plots were presented, the median and interquartile range were extracted and transformed (50, 51). SE or 95% CI, if provided, were transformed into SD values (52). In total, 3,286 effect size measures were obtained.

Publication bias and sensitivity analysis. The databases are robust and free from publication bias, as indicated by the results of Egger's (for terrestrial and freshwater ecosystems) or Begg's (for terrestrial and marine ecosystems) regression tests (*SI Appendix*, Fig. S13). The evidence for minimal publication bias was further substantiated by the Rosenthal's fail-safe-number test (53), indicating that tens of thousands of publications would be required to reduce the observed significance (*SI Appendix*, Fig S13). In the leave-one-out sensitivity analysis, each data point contributed to the overall outcome consistently (54) (Dataset S2). More information is given in *SI Appendix*, Text S6.

Effect size calculation. We categorized the effect size of the response to MP exposure into six different main groups: i) total chlorophyll content; ii) chlorophyll *a* content; iii) chlorophyll *b* content; iv) carotenoid content; v) maximum quantum efficiency of photosystem II (Fv/Fm ratio); and vi) the spectral global quantum yield of photosystem II (YII).

To quantify the effect of MP exposure on photosynthesis performance (the effect size), the natural logarithmic of the response ratio $\left(\ln(RR)\right)$ (55) was employed as follows:

$$\ln(RR) = \ln\left(R_{exp}/R_{cont}\right), \quad [1]$$

where R_{exp} and R_{cont} represent responses of the exposed and control groups, respectively. Considering potential bias when sample sizes are small, or when SD and means are of similar magnitude (56), we utilized bias-corrected estimators to calculate natural log-transformed response ratios $\left(\ln\left(RR^{w}\right)\right)$ of each piece of data and their variances (57) in this study as follows:

$$\ln\left(RR^{w}\right) = \ln\left(R_{exp}/R_{cont}\right) + \frac{1}{2}\left[\frac{\left(SD_{exp}\right)^2}{\left(n_{exp}\times R_{exp}^2\right)} - \frac{\left(SD_{cont}\right)^2}{\left(n_{cont}\times R_{cont}^2\right)}\right], \quad [2]$$

$$\mathrm{Var}\left[\ln\left(RR^{w}\right)\right] = \left[\frac{\left(SD_{exp}\right)^2}{\left(n_{exp}\times R_{exp}^2\right)} - \frac{\left(SD_{cont}\right)^2}{\left(n_{cont}\times R_{cont}^2\right)}\right] + \frac{1}{2}\left[\frac{\left(SD_{exp}\right)^4}{\left(n_{exp}^2\times R_{exp}^4\right)} - \frac{\left(SD_{cont}\right)^4}{\left(n_{cont}^2\times R_{cont}^4\right)}\right], \quad [3]$$

where n_{exp} and n_{cont} are the sample sizes of the exposed and control groups, respectively, and SD_{exp} and SD_{cont} are the SD of the exposed and control groups, respectively. The overall effects in photosynthesis main groups (e.g., total chlorophyll content, chlorophyll *a* content, etc.), MP characteristics (e.g., size), and exposure conditions (e.g., exposure duration and concentration) were assessed by the likelihood ratio tests in a mixed-effect multivariate model (58) (*SI Appendix*, Table S1). The meta-analysis was conducted with RStudio in R version 4.0.3 with the "meta", "metafor", "lme4", "nlme", "ggplot2," and "multcomp" packages. The forest plot was visualized using Origin 2023 and Adobe Illustrator 2023.

ML and Effect Size Prediction. Five frequently used ML models (Elastic Net regression, K-Nearest Neighbors, Support Vector Regression, RF, and eXtreme Gradient Boosting) were employed to construct the model (*SI Appendix*, Fig. S3). The RF model demonstrated the best performance was selected for parameter interpretation and prediction (Fig. 2). Briefly, a summary dataset was generated by combining the datasets of the terrestrial, marine, and freshwater ecosystems from the meta-analysis, and then randomly divided into an 80% training dataset and a 20% test dataset with a one-time random seed (three seeds were used to obtain the averages). The training set was used to optimize the hyperparameters and reduce overfitting risk by conducting fivefold cross validation using Bayesian optimization algorithm, and the test dataset was used to quantify the model performance. The evaluation metrics for the predictive performance were mean R^2, RMSE, and MAE (59). The ML models were implemented using the scikit-learn 1.2.2 package in Python 3.8.8. The importance and contributions of parameters affecting the RF model output were assessed using the SHAP method, specifically the SHAP 0.41.0 analysis.

We also collected data from the literature on environmental MP levels in terrestrial, marine, and freshwater ecosystems in Europe and North America. These regions are of significance in the production and utilization of plastics (60), yet they contribute to less than 20% of the existing meta-analysis dataset (*SI Appendix*, Table S10). The resulting effect sizes were predicted using the constructed RF model, as shown in *SI Appendix*, Table S7. The origins of uncertainties in our model are discussed at length in *SI Appendix*, Text S5.

Estimate of Global Primary Productivity and Food Production Losses.

SCOPE model and input parameters. SCOPE model describes radiative transfer processes and exchanges of energy fluxes, carbon, and water among the soil, vegetation, and the atmosphere (61–63). It integrates radiative transfer processes within leaves and vegetation canopies based on photosynthesis processes and energy balance. The model demonstrates a high level of performance in simulating GPP when validated against field data (62). In this work, the loss of GPP (GPP_{loss}) following MP exposure was calculated as the difference of GPP without (GPP_{ref}) and with (GPP_{exp}) MP exposure:

$$GPP_{loss} = GPP_{ref} - GPP_{exp}, \quad [4]$$

where GPP_{ref} was calculated employing the SCOPE model on a pixel basis (0.083°×0.083°) globally, with incoming short-radiation and air temperature from ERA5 reanalysis data (64), leaf area index (*LAI*) from Copernicus (65), leaf total chlorophyll content (*Cab*) (66), and leaf maximum carboxylation rate (V_{cmax}) (67). Other parameters were set as their default values (68). GPP_{exp} was estimated using the SCOPE model with corrected input data (including *LAI*, *Cab*, and V_{cmax}) using a correction factor of *k* (%, decrease in these parameters upon MP exposure, *SI Appendix*, Table S8):

The global crop production losses with MP exposure ($Crop_{loss}$) were thus estimated by employing the global crop production without MP exposure ($Crop_{ref}$) using Eq. **5**:

$$\frac{Crop_{loss}}{Crop_{ref}} = \frac{GPP_{loss}}{GPP_{ref}}, \quad [5]$$

where the $Crop_{ref}$ for the 2020 version was obtained from the SPAM (69). The Matlab R2023a and Arcmap 10.8 were utilized to carry out model operations and visualize data.

VGPM and input parameters. A standard VGPM was employed to estimate the average annual NPP losses of GAEs (70). VGPM is one of the most widely used models for estimating NPP from satellite ocean color remote sensing (71). The NPP losses of GAEs ($NPP_{GAEs}loss$) upon MP exposure were calculated as the difference of NPP without (NPP_{ref}) and with (NPP_{exp}) MP exposure:

$$NPP_{GAEs}loss = NPP_{ref} - NPP_{exp}, \quad [6]$$

where NPP_{ref} was estimated utilizing the VGPM in combination with data collected by the MODIS sensor, with the calculation formula presented in Eq. **7**:

$$NPP_{ref} = 0.0615 \times P^B_{opt} \times \left(\frac{E_0}{E_0 + 4.1}\right) \times Z_{eu} \times Chla \times D_{irr}, \quad [7]$$

where E_0 represents the daily photosynthetically available radiation at the surface, Z_{eu} denotes the euphotic-zone depth where the solar radiation is 1% of its surface value, *Chla* represents the surface chlorophyll *a* concentration, D_{irr} indicates the photoperiod (72). The P^B_{opt} is the optimal assimilation efficiency of the productivity profile, which is derived from an empirically parameterized sea surface temperature (*SST*) dependent polynomial (71, 73). All input data pertaining to Eq. **7** (excluding P^B_{opt}) and *SST* can be obtained up to 2022 through satellite retrieval and downloaded from the Ocean Productivity database (74).

NPP_{exp} was calculated in a manner analogous to NPP_{ref} through the application of Eq. **8**, with *Chla* modified using a correction factor of *k* (%, decrease in *Chla* upon MP exposure, summarized in *SI Appendix*, Table S8):

$$NPP_{exp} = 0.0615 \times P^B_{opt} \times \left(\frac{E_0}{E_0 + 4.1}\right) \times Z_{eu} \times (1+k) Chla \times D_{irr}, \quad [8]$$

The model operation and data visualization were implemented by Matlab R2023a and Adobe Illustrator 2023. More details can be found in *SI Appendix*, Text S7.

Transformation of fish and seafood losses. Pauly and Christensen (75) proposed the method to quantify the primary productivity required (*PPR*) for fishery catches (76):

$$PPR = \sum_{i=1}^{n} \frac{C_i}{CR} \times \left(\frac{1}{TE}\right)^{(TL_i - 1)}, \quad [9]$$

where C_i refers to the fishery catches of aquatic species *i*, TL_i represents the trophic level of aquatic species *i*, *CR* denotes the conversion rate of wet weight to carbon (9:1) (76), *TE* is the trophic transfer efficiency in the aquatic ecosystems (10%) (75). All input data were available through Sea Around Us project (77).

Fishery catches losses under MP exposure could thus be estimated using Eq. **9** and the NPP losses. Following the calculation of global fishery losses, global fish and seafood losses and the amount of these resources used for human consumption could be calculated based on the data provided by the FAO (78). Please refer to *SI Appendix*, Text S7 and Table S5 for more details. Microsoft Excel 2021, Origin 2023, and Adobe Illustrator 2023 were utilized to process and visualize the data.

Prospect of global food supply and demand. Projected food supply and demand were estimated under two different scenarios: the business-as-usual scenario and the MP exposure scenario. The projected food supply in the business-as-usual scenario between 2030–2050 was obtained from the FAO (79). In parallel, the projected food supply under the MP exposure scenario was estimated as the difference between the projected food supply in the business-as-usual scenario and the aforementioned food production losses upon MP exposure. Projected food demand was estimated by multiplying the projected total global population, obtained from the UN Probabilistic Population Projections (80), by the per capita food demand, obtained from the latest FAO data (*SI Appendix*, Fig. S7*B*).

The projected net increase in the global population at risk of hunger from 2030 to 2050 upon MP exposure was calculated as the difference between the aforementioned projected total global population obtained from the UN Probabilistic Population Projections (80) and the projected global population (*Pop*(*sustain*)) that can be sustained by the global food production under MP exposure. *Pop*(*sustain*) was estimated using Eq. **10**:

$$Pop(sustain) = \frac{Food(FAO) - Food(loss)}{Food(percapitademand)}. \quad [10]$$

Where *Food*(*FAO*) indicates the projected total production of three main crops by the FAO (79), *Food*(*loss*) represents the estimated production losses under MP exposure (Fig. 3), and *Food*(*percapitademand*) is the per capita food demand

(*SI Appendix*, Fig. S7*B*). Microsoft Excel 2021, Origin 2023, and Adobe Illustrator 2023 were utilized for raw data processing and visualization.

Estimation of Reductions in Photosynthesis Losses Under MP Mitigation Scenarios. Reductions in photosynthesis losses in response to MP mitigation were estimated as the difference between the photosynthesis losses under MP mitigation projections (based on constructed RF model; see *Materials and Methods*) and those under the business-as-usual scenario (based on meta-analysis, see *Materials and Methods* and *SI Appendix*, Text S4). A range of MP mitigation scenarios, i.e., business-as-usual, lower projections (1 to 20%), intermediate projections (21 to 40%), and higher projections (41 to 50%), were established in various ecosystems based on published literatures that report, estimate, or project reductions in plastic use and discharge, as well as efficiencies of plastic residue degradation (summarized in *SI Appendix*, Table S6). The estimated reductions in photosynthesis losses were then fed into the SCOPE model and VGPM to assess the reductions in losses of main crops (rice, wheat, and maize), global aquatic NPP, seafood, and protein, as described above. Furthermore, the decline in the value of agricultural production of rice, wheat, and maize was estimated by multiplying the reductions in their loss percentages by their respective FAO values of agricultural production (81). The Microsoft Excel 2021, Origin 2023, and Matlab R2023a were utilized for raw data processing and visualization.

Data, Materials, and Software Availability. All study data are included in the article and/or supporting information.

ACKNOWLEDGMENTS. This work was supported by the National Key R&D Program of China (2023YFC3711400), the National Natural Science Foundation of China (42222702), the Basic Science Center Project of the National Natural Science Foundation of China (52388101), and the NSF of Jiangsu Province (BK20220092). We thank the reviewers for their valuable comments and suggestions, which have greatly improved the quality of this study.

Author affiliations: [a]State Key Laboratory of Pollution Control and Resources Reuse, School of the Environment, Nanjing University, Nanjing 210023, China; [b]International Institute for Earth System Sciences, Jiangsu Center for Collaborative Innovation in Geographical Information Resource Development and Application, Nanjing University, Nanjing 210023, China; [c]Jiangsu Provincial Key Laboratory of Geographic Information Science and Technology, Key Laboratory for Land Satellite Remote Sensing Applications of Ministry of Natural Resources, School of Geography and Ocean Science, Nanjing University, Nanjing 210023, China; [d]International Joint Carbon Neutrality Laboratory, Nanjing University, Nanjing 210023, China; [e]State Key Laboratory of Soil and Sustainable Agriculture, Institute of Soil Science, Chinese Academy of Sciences, Nanjing 211135, China; [f]University of Chinese Academy of Sciences, Beijing 100049, China; [g]Institute of Environmental Research at Greater Bay Area, Key Laboratory for Water Quality and Conservation of the Pearl River Delta, Ministry of Education, Guangzhou University, Guangzhou 510006, China; [h]State Key Laboratory of Estuarine and Coastal Research, East China Normal University Shanghai, Shanghai 200241, China; [i]Institute of Biology, Freie Universität Berlin, Berlin 14195, Germany; [j]Berlin-Brandenburg Institute of Advanced Biodiversity Research, Berlin 14195, Germany; and [k]Stockbridge School of Agriculture, University of Massachusetts, Amherst, MA 01003

Author contributions: R.Z., H.Z., and F.D. designed research; R.Z., Z.Z., N.Z., and F.D. performed research; Z.Z., C. Liu, F.D., and Y.Z. contributed new reagents/analytic tools; R.Z., Z.Z., and N.Z. analyzed data; H.Z. and F.D. conceptualization, project administration, supervision; R.Z., F.Z., X.Z., Y.H., and Y.Y. data collection; H.Z., C. Liu, Y.W., C. Li, H.S., M.C.R., F.D., H.R., Y.Z., and B.X. paper review and editing; and R.Z., Z.Z., H.Z., and F.D. wrote the paper.

1. FAO, *World Food and Agriculture – Statistical Yearbook 2022* (Food & Agriculture Org., Rome, 2022).
2. G. V. Lowry *et al.*, Towards realizing nano-enabled precision delivery in plants. *Nat. Nanotechnol.* **19**, 1255–1269 (2024).
3. On the plastics crisis, *Nat. Sustainability* **6**, 1137–1137 (2023).
4. FAO, *Assessment of Agricultural Plastics and Their Sustainability* (A call for action, Rome, 2021).
5. B. Speißer, R. A. Wilschut, M. van Kleunen, Number of simultaneously acting global change factors affects composition, diversity and productivity of grassland plant communities. *Nat. Commun.* **13**, 7811 (2022).
6. J. K. Moore *et al.*, Sustained climate warming drives declining marine biological productivity. *Science* **359**, 1139–1143 (2018).
7. W. R. Wieder, C. C. Cleveland, W. K. Smith, K. Todd-Brown, Future productivity and carbon storage limited by terrestrial nutrient availability. *Nat. Geosci.* **8**, 441–444 (2015).
8. S. K. Kim *et al.*, Arctic Ocean sediments as important current and future sinks for marine microplastics missing in the global microplastic budget. *Sci. Adv.* **9**, eadd2348.
9. R. Shi *et al.*, Toxicity mechanisms of nanoplastics on crop growth, interference of phyllosphere microbes, and evidence for foliar penetration and translocation. *Environ. Sci. Technol.* **58**, 1010–1021 (2023).
10. Y. Wang *et al.*, Positively charged microplastics induce strong lettuce stress responses from physiological, transcriptomic, and metabolomic perspectives. *Environ. Sci. Technol.* **56**, 16907–16918 (2022).
11. X. D. Sun *et al.*, Differentially charged nanoplastics demonstrate distinct accumulation in *Arabidopsis thaliana*. *Nat. Nanotechnol.* **15**, 755–760 (2020).
12. M. S. Bank, D. M. Mitrano, M. C. Rillig, C. Sze Ki Lin, Y. S. Ok, Embrace complexity to understand microplastic pollution. *Nat. Rev. Earth Environ.* **3**, 736–737 (2022).
13. M. Helal, N. B. Hartmann, F. R. Khan, E. G. Xu, Time to integrate "One Health Approach" into nanoplastic research. *Eco-Environ. Health* **2**, 18–20 (2023).
14. L. Chen *et al.*, A machine learning model that outperforms conventional global subseasonal forecast models. *Nat. Commun.* **15**, 6425 (2024).
15. S. Zhong *et al.*, Machine learning: New ideas and tools in environmental science and engineering. *Environ. Sci. Technol.* **55**, 12741–12754 (2021).
16. X. Jia, T. Wang, H. Zhu, Advancing computational toxicology by interpretable machine learning. *Environ. Sci. Technol.* **57**, 17690–17706 (2023).
17. S. Wang *et al.*, Estimation of leaf photosynthetic capacity from leaf chlorophyll content and leaf age in a subtropical evergreen coniferous plantation. *J. Geophys. Res. Biogeosci.* **125**, e2019JG005020 (2020).
18. A. Porcar-Castell *et al.*, Chlorophyll a fluorescence illuminates a path connecting plant molecular biology to Earth-system science. *Nat. Plants* **7**, 998–1009 (2021).
19. P. H. Raven, R. F. Evert, S. E. Eichhorn, *Raven Biology of Plants.* 8th edn. **7**, 122–155 (W.H. Freeman and Company, 2013).
20. E. Prikaziuk, M. Migliavacca, Z. Su, C. van der Tol, Simulation of ecosystem fluxes with the SCOPE model: Sensitivity to parametrization and evaluation with flux tower observations. *Remote Sens. Environ.* **284**, 113324 (2023).
21. D. Treutter, Significance of flavonoids in plant resistance: A review. *Environ. Chem. Lett.* **4**, 147–157 (2006).
22. R. Matyssek *et al.*, Growth and parasite defence in plants; The balance between resource sequestration and retention: In lieu of a guest editorial. *Plant Biol.***4**, 133–136 (2002).
23. J. R. Jambeck *et al.*, Plastic waste inputs from land into the ocean. *Science* **347**, 768–771 (2015).
24. G. G. Deme *et al.*, Macro problems from microplastics: Toward a sustainable policy framework for managing microplastic waste in Africa. *Sci. Total Environ.* **804**, 150170 (2022).
25. E. S. Okeke *et al.*, Microplastic burden in Africa: A review of occurrence, impacts, and sustainability potential of bioplastics. *Chem. Eng. J. Adv.* **12**, 100402 (2022).
26. S. Peng *et al.*, Rice yields decline with higher night temperature from global warming. *Proc. Natl. Acad. Sci. U.S.A.* **101**, 9971–9975 (2004).
27. D. B. Lobell, W. Schlenker, J. Costa-Roberts, Climate trends and global crop production since 1980. *Science* **333**, 616–620 (2011).
28. C. Lesk, P. Rowhani, N. Ramankutty, Influence of extreme weather disasters on global crop production. *Nature* **529**, 84–87 (2016).
29. J. Fu *et al.*, Extreme rainfall reduces one-twelfth of China's rice yield over the last two decades. *Nat. Food* **4**, 416–426 (2023).
30. Q. Zhang *et al.*, Divergent effectiveness of irrigation in enhancing food security in droughts under future climates with various emission scenarios. *npj Clim. Atmos. Sci.* **6**, 40 (2023).
31. FAO, Ifad, UNICEF, WFP and WHO, *The State of Food Security and Nutrition in the World, Urbanization, Agrifood Systems Transformation and Healthy Diets across The Rural–urban Continuum* (FAO, Rome, 2023).
32. F. Dang, Q. Wang, Y. Huang, Y. Wang, B. Xing, Key knowledge gaps for one health approach to mitigate nanoplastic risks. *Eco-Environ. Health* **1**, 11–22 (2022).
33. L. J. W. van der Laan, T. Bosker, W. J. G. M. Peijnenburg, Deciphering potential implications of dietary microplastics for human health. *Nat. Rev. Gastroenterol. Hepatol.* **20**, 340–341 (2023).
34. L. Cao *et al.*, Vulnerability of blue foods to human-induced environmental change. *Nat. Sustainability* **6**, 1186–1198 (2023).
35. T. Marshall, Dietary guidelines for Americans, 2010. *J. Am. Dental Assoc.* **142**, 654–656 (2011).
36. WHO, Fao, UNU, *Protein and Amino Acid Requirements in Human Nutrition in Report of A Joint FAO/WHO/UNU Expert Consultation Technical Report Series No 935* (WHO, Geneva, 2007).
37. J. Z. Koehn, J. P. Leape, E. H. Allison, Aquatic foods at the nutrition–environment nexus. *Nat. Sustainability* **6**, 1497–1498 (2023).
38. R. Manu *et al.*, Response of tropical forest productivity to seasonal drought mediated by potassium and phosphorus availability. *Nat. Geosci.* **17**, 524–531 (2024).
39. C. Plaza *et al.*, Ecosystem productivity has a stronger influence than soil age on surface soil carbon storage across global biomes. *Commun. Earth Environ.* **3**, 233 (2022).
40. L. Yang, X. He, S. Ru, Y. Zhang, Herbicide leakage into seawater impacts primary productivity and zooplankton globally. *Nat. Commun.* **15**, 1783 (2024).
41. E. Y. Kwon *et al.*, Nutrient uptake plasticity in phytoplankton sustains future ocean net primary production. *Sci. Adv.* **8**, eadd2475 (2022).
42. A. Ortega *et al.*, Important contribution of macroalgae to oceanic carbon sequestration. *Nat. Geosci.* **12**, 748–754 (2019).
43. R. M. Thompson *et al.*, Food webs: Reconciling the structure and function of biodiversity. *Trends in Ecol. Evol.* **27**, 689–697 (2012).
44. A. P. K. Tai, M. V. Martin, C. L. Heald, Threat to future global food security from climate change and ozone air pollution. *Nat. Clim. Change* **4**, 817–821 (2014).
45. R. C. Henry *et al.*, Global and regional health and food security under strict conservation scenarios. *Nat. Sustainability* **5**, 303–310 (2022).
46. L. Jia, S. Evans, S. v. d. Linden, Motivating actions to mitigate plastic pollution. *Nat. Commun.* **10**, 4582 (2019).
47. C. Morales-Caselles *et al.*, An inshore–offshore sorting system revealed from global classification of ocean litter. *Nat. Sustainability* **4**, 484–493 (2021).
48. UN, What is the Triple Planetary Crisis? (2022), https://unfccc.int/news/what-is-the-triple-planetary-crisis. Accessed 17 August 2024.
49. C. Li, H. Zhong, How to clear the obstacles blocking uptake of a global plastic treaty. *Nature*, (2025) in press.
50. J. Shi *et al.*, Optimally estimating the sample standard deviation from the five-number summary. *Res. Synth. Methods* **11**, 641–654 (2020).
51. J. Shi *et al.*, Detecting the skewness of data from the five-number summary and its application in meta-analysis. *Stat. Methods Medical Res.* **32**, 1338–1360 (2023).
52. F. Dang *et al.*, Threats to terrestrial plants from emerging nanoplastics. *ACS Nano.* **16**, 17157–17167 (2022).

53. W. Viechtbauer, Publication bias in meta-analysis: Prevention, assessment and adjustments. *Psychometrika* **72**, 269–271 (2007).
54. M. B. Mathur, T. J. VanderWeele, Sensitivity analysis for publication bias in meta-analyses. *J. R. Stat. Soc. Series C. Appl. Stat.* **69**, 1091–1119 (2020).
55. L. V. Hedges, J. Gurevitch, P. S. Curtis, The meta-analysis of response ratios in experimmental ecology. *Ecology* **80**, 1150–1156 (1999).
56. J. Gurevitch, J. Koricheva, S. Nakagawa, G. Stewart, Meta-analysis and the science of research synthesis. *Nature* **555**, 175–182 (2018).
57. M. J. Lajeunesse, Bias and correction for the log response ratio in ecological meta-analysis. *Ecology* **96**, 2056–2063 (2015).
58. D. Hu, C. Wang, A. M. O'Connor, A likelihood ratio test for the homogeneity of between-study variance in network meta-analysis. *Syst. Rev.* **10**, 310 (2021).
59. J. Yan, X. Yan, S. Hu, H. Zhu, B. Yan, Comprehensive interrogation on acetylcholinesterase inhibition by ionic liquids using machine learning and molecular modeling. *Environ. Sci. Technol.* **55**, 14720–14731 (2021).
60. Plastic Europe, Plastics – the fast facts 2023. https://plasticseurope.org/knowledge-hub/plastics-the-fast-facts-2023/. Accessed: July 2024.
61. C. van der Tol, W. Verhoef, A. Rosema, A model for chlorophyll fluorescence and photosynthesis at leaf scale. *Agricul. Forest Meteorol.* **149**, 96–105 (2009).
62. C. van der Tol *et al.*, A model and measurement comparison of diurnal cycles of sun-induced chlorophyll fluorescence of crops. *Remote Sens. Environ.* **186**, 663–677 (2016), 10.1016/j.rse.2016.09.021.
63. C. van der Tol, J. A. Berry, P. K. E. Campbell, U. Rascher, Models of fluorescence and photosynthesis for interpreting measurements of solar-induced chlorophyll fluorescence. *J. Geophys. Res. Biogeosci.* **119**, 2312–2327 (2014).
64. Programme of the European Union, Climate data store. ERA5 hourly data on single levels from 1940 to present. (1940), 10.24381/cds.adbb2d47. Accessed: August 2024.
65. Copernicus, CLMS portfolio vegetation. https://land.copernicus.eu/global/products/lai. Accessed: August 2024.
66. M. Xu *et al.*, Retrieving global leaf chlorophyll content from MERIS data using a neural network method. *ISPRS J. Photogram. Remote Sens.* **192**, 66–82 (2022).
67. Y. Liu *et al.*, Global photosynthetic capacity of C3 biomes retrieved from solar-induced chlorophyll fluorescence and leaf chlorophyll content. *Remote Sens. Environ.* **287**, 113457 (2023).
68. C. van der Tol, W. Verhoef, J. Timmermans, A. Verhoef, Z. Su, An integrated model of soil-canopy spectral radiances, photosynthesis, fluorescence, temperature and energy balance. *Biogeosciences* **6**, 3109–3129 (2009).
69. M. Lu *et al.*, A cultivated planet in 2010 – Part 1: The global synergy cropland map. *Earth Syst. Scientif. Data* **12**, 1913–1928 (2020).
70. B. Ping, Y. Meng, C. Xue, F. Su, Oceanic primary production estimation based on machine learning. *J. Geophys. Res. Oceans* **128**, e2022JC018980 (2023).
71. M. J. Behrenfeld, P. G. Falkowski, A consumer's guide to phytoplankton primary productivity models. *Limnol. Oceanogr.* **42**, 1479–1491 (1997).
72. L. Song *et al.*, On the spatial and temporal variations of primary production in the South China Sea. *IEEE Transac. Geosci. Remote Sens.* **61**, 1–14 (2023).
73. K. W. Lan, L. J. Lian, C. H. Li, P. Y. Hsiao, S. Y. Cheng, Validation of a primary production algorithm of vertically generalized production model derived from multi-satellite data around the waters of Taiwan. *Remote Sens.* **12**, 1627 (2020).
74. Ocean Productivity, Standard VGPM http://orca.science.oregonstate.edu/npp_products.php.
75. D. Pauly, V. Christensen, Primary production required to sustain global fisheries. *Nature* **374**, 255–257 (1995).
76. E. Chassot *et al.*, Global marine primary production constrains fisheries catches. *Ecol. Lett.* **13**, 495–505 (2010).
77. Sea Around Us, Tools & data. Net parimary production of Large marine ecosystems. https://www.seaaroundus.org/. Accessed: July 2024.
78. FAO, Fisheries and aquaculture. FishStat. https://www.fao.org/fishery/en/fishstat. Accessed: June 2024.
79. FAO, Global perspectives studies. Food and agriculture projections to 2050. https://www.fao.org/global-perspectives-studies/food-agriculture-projections-to-2050/en. Accessed: June 2024.
80. UN, World population prospects 2024. https://population.un.org/wpp/. Accessed: June 2024.
81. FAO. FAOSTAT, Production value of agricultural production. https://www.fao.org/faostat/en/#data/QV. Accessed: July 2024.